

MAGNETIC RESONANCE IMAGING IN THE DIAGNOSIS OF MALIGNANT TUMORS OF THE MAXILLOFACIAL REGION

Dijana Podoreški¹, Ivan Krolo¹, Mirko Ivkić², Miljenko Marotti¹, Vilma Kosović¹ and Klaudija Višković³

¹University Department of Diagnostic and Interventional Radiology, ²University Department of ENT, Head and Neck Surgery, Sestre milosrdnice University Hospital; ³Department of Radiology and Ultrasonography, Dr. Fran Mihaljević University Hospital for Infectious Diseases, Zagreb, Croatia

SUMMARY – Magnetic resonance imaging (MRI) is a radiological imaging method that has not yet found routine application in the detection and assessment of malignant tumors of the maxillofacial region. The aim of this study was to evaluate MRI in the detection, diagnosis and differential diagnosis of malignant tumors of the maxillofacial region. This prospective study included 42 patients with clinically confirmed malignant tumors of the maxillofacial region. All patients were examined by MRI. This imaging method was evaluated for the ability to detect tumor location and to analyze dimensions and structure of the tumor, bone involvement, effect on neurovascular structures and extension to soft tissues. MRI results were compared with histopathologic and intraoperative findings as the 'gold standard' methods. MRI identified all of the clinically confirmed tumors. The sensitivity for tumor location was 94.4%, tumor necrosis 93%, hemorrhage 93.3% and bone involvement 91.4%. The specificity for tumor location was 84%, tumor necrosis 92.8%, hemorrhage 92.8% and bone involvement 85.7%. In the evaluation of soft tissue tumor extension to bone structures, MRI sensitivity and specificity was 94.4% and 88.2%, respectively. The sensitivity for perineural infiltration and tumor involvement of vascular structures was 91% and 91.6%, respectively. The specificity for perineural infiltration was 96.7% and for tumor involvement of vascular structures 88%. MRI sensitivity and specificity for intracranial extension, intraorbital propagation, extension to pterygopalatine fossa and other surrounding anatomic spaces was 93.5% and 90.9%, respectively. MRI proved advantageous for the ability to distinguish neurovascular structures from adjacent soft tissues without the use of intravenous contrast media. Study results demonstrated MRI to provide valuable information in the analysis of tumor structure, bone involvement and extension to soft tissues of malignant tumors of the maxillofacial region.

Key words: *Maxillary neoplasms – radiography, diagnosis; Magnetic resonance imaging – utilization; Neoplasms invasion – diagnosis*

Introduction

Malignant tumors of the maxillofacial region include many different types of tumors. According to

Correspondence to: *Dijana Podoreški, MD*, University Department of Diagnostic and Interventional Radiology, Sestre milosrdnice University Hospital, Vinogradska c. 29, HR-10000 Zagreb, Croatia

E-mail: podoreski@sfzg.hr

Received January 25, 2010, accepted February 26, 2010

the World Health Organization (WHO), head and neck tumors are anatomically classified into several groups: nasal cavity and paranasal sinuses, nasopharynx, hypopharynx, larynx and trachea, oral cavity and oropharynx, salivary glands, odontogenic tumors, and ear and paraganglionic system¹.

Malignant tumors of the mandible and maxilla are grouped into primary tumors that originate within the mandible and maxilla and secondary tumors that in-

volve the mandible and maxilla secondarily. The most common malignant tumors of the mandible include squamous cell carcinoma (SCC) of the oral cavity, i.e. SCC of the gingival mandible and floor of the mouth that invade the mandible secondarily². Metastatic tumors are not uncommon malignant lesions in the mandible. Tobacco and alcohol consumption are the most common predisposing factors². SCC accounts for more than 95% of the tumors that arise from oral mucosa³. In the nasal cavity, 85% of SCC occur in the lateral wall and floor³. Carcinoma of the septum is felt to be rare. Eighty percent of paranasal sinus SCC occur in the maxillary antrum³. Adenoid cystic carcinoma of the sinonasal region is a rare cancer that accounts for 10% of all malignancies at this site⁴. Sinonasal adenocarcinoma typically arises from the middle turbinate or ethmoid sinus and less commonly from the antrum¹. Adenocarcinoma occurs predominantly in men and is associated with wood dust exposure¹. Nearly 20% of malignant melanomas in the human body occur in the head and neck, and the face represents 3.5% of total body surface⁵.

About 10% of osteosarcoma cases occur in the head and neck region, with the majority involving the mandible¹. The maxilla is the second most common head and neck site, however, cases of the maxillary and ethmoid sinus involvement have also been reported⁶. In the mandible, osteosarcoma accounts for about 4% of all primary malignant tumors⁷. Bone involvement shows highest incidence in the second decade of life. The etiology and precise pathogenesis of the disease remain unknown⁷. Chondrosarcoma is a malignant tumor of cartilage that rarely involves the sinonasal region⁸. Esthesioneuroblastoma is a rare, malignant neoplasm arising from the olfactory neuroepithelium in the upper nasal cavity¹.

Patients and Methods

This prospective study included 42 patients with clinically confirmed malignant tumors of the maxillofacial region. All patients were examined by magnetic resonance imaging (MRI; Siemens Magnetom Avanto, 1.5 Tesla, Berlin, Germany) at University Department of Diagnostic and Interventional Radiology, Sestre milosrdnice University Hospital in Zagreb between May 2007 and December 2009.

MRI was performed using standard head coil to obtain T1-weighted images with and without contrast medium and T2-weighted images in axial, coronal and sagittal planes; T1-weighted images with fat saturation and contrast media (FS-T1) and Short Tau Inversion Recovery T2-weighted images (STIR-T2) in coronal planes. For T1-weighted images the field of view (FOV) was 210–230 mm and for T2-weighted images and STIR-T2 it was 130–200 mm, with matrix size of 256x256 pixels. Section thickness varied from 1 to 3 mm and each patient received the paramagnetic contrast medium, gadolinium-diethylenetriamine penta-acetic acid (Gd-DTPA) in a dose of 0.1 mmol/kg. Data were archived in picture archiving and communication systems (PACS).

The images were evaluated for tumor location and dimensions. We analyzed structural homogeneities and inhomogeneities, and detected zones of necrosis and hemorrhage. Bone involvement analysis included osteosclerosis, osteolysis, cortical expansion, and cortical thinning or destruction. Soft tissue tumors were analyzed for their extension to cortical bone and bone marrow. Tumor extension to soft tissues was considered as involvement of the adjacent neurovascular structures, fat tissue, muscles and anatomic spaces.

MRI findings were compared with histopathologic and intraoperative findings as the 'gold standard' methods.

The specificity and sensitivity were analyzed by statistical processing of the results. Sensitivity was defined as the ability of MRI to detect the presence of pathology and was calculated as follows¹⁹:

$$\text{Sensitivity} = ((\text{True Positive} / (\text{True Positive} + \text{False Negative})) \times 100).$$

Specificity was defined as the ability of imaging to detect the absence of pathology and was calculated as follows:

$$\text{Specificity} = ((\text{True Negative} / (\text{True Negative} + \text{False Negative})) \times 100).$$

Results

Tumor pathology was found in 18 female and 24 male patients, mean age 62.3 and 57.3 years, respectively. The youngest patient was a 20-year-old man with osteosarcoma of the mandible, and the oldest was an 80-year-old man with adenocarcinoma of the nasal cavity. The smallest tumor measured 15 mm

Table 1. Histopathologic findings of the tumors (N=42)

Histopathology	Number of patients	%
Sublingual SCC	6	14.3
SCC of maxillary sinus	5	11.9
SCC of ethmoid sinus	2	4.8
SCC of gingival maxilla	7	16.6
SCC of gingival mandible	9	21.4
SCC of gingival maxilla and hard palate	2	4.8
Adenocarcinoma of nasal fossa	5	11.9
Osteosarcoma of mandible	5	11.9
Malignant melanoma	1	2.4

SCC = squamous cell carcinoma

and the largest tumor measured 65 mm in longest diameter, yielding a mean tumor diameter of 34 mm. Histopathologic findings of the tumors are shown in Table 1.

In the evaluation of tumor location, MRI showed 94.4% sensitivity and 84% specificity. Tumor location was presented in sagittal scan, on a T1-weighted image (Fig. 1) (sinonasal adenocarcinoma located in the nasal fossa, typically arising from the middle turbinate).



Fig. 1. Sagittal contrast-enhanced T1-weighted image shows sinonasal adenocarcinoma located in the nasal fossa, typically arising from the middle turbinate (white arrows).

range of deviation was 4 mm (minimum – 2 mm and maximum 2 mm). Study results showed a limitation of MRI on measuring the height and width of tumor lesion. The main reasons were smaller artifact disturbances from dental restorative materials. On measuring tumor depth, the absolute range of deviation was 14 mm (minimum – 3 and maximum 11). The heavy horizontal artifacts were the reason for MRI limitation on evaluating tumor depth. In one patient, the measurement error was 11 mm.

MRI analysis of tumor structure showed structural homogeneities in seven patients. Tumors with zones of necrosis were found in 26 patients, whereas 20 patients had tumors with zones of hemorrhage, which was in accordance with histopathologic and intraoperative findings. The sensitivity and specificity of MRI on detecting necrotic zones was 93% and 92.8%, and for hemorrhage 93.3% and 92.8%, respectively.

Thirty seven patients had tumors originating in soft tissue structures, including SCC of the oral cavity (n=6), SCC of the gingival maxilla (n=7), SCC of the gingival mandible (n=9), SCC of the gingival maxilla and hard palate (n=2), SCC of the maxillary and ethmoid sinuses (n=7), sinonasal adenocarcinoma (n=5) and malignant melanoma (n=1). We analyzed cortical and bone marrow extension of the tumor. MRI detected the extension of soft tissue tumors to bone structures with 94.4% sensitivity and 88.2% specificity. Five patients had osteosarcoma of the mandible. Bone involvement analysis included osteosclerosis, osteolysis, cortical expansion, and cortical thinning or destruction. MRI sensitivity for bone involvement was 91.4% and specificity 85.7% (Figs. 2-4).

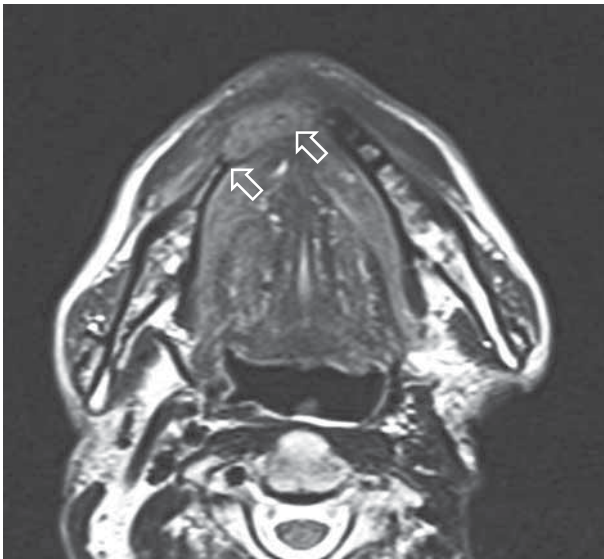


Fig. 2. Axial T2-weighted image shows destruction of the mandible, interrupted corticalis and intramedullary tumor extension (white arrows). Histopathology confirmed ulcerative squamous cell carcinoma of the gingival mandible.

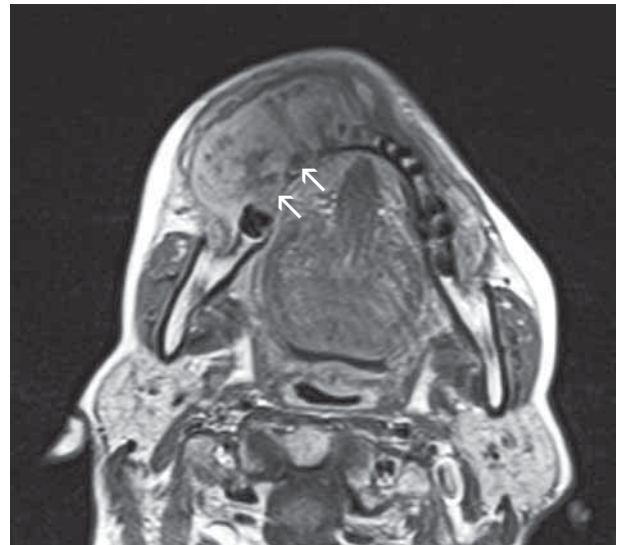


Fig. 4. Axial contrast-enhanced T1-weighted image shows osteosarcoma of the mandible. Inhomogeneous well contrast-enhanced tumor mass with osteosclerosis, interrupted cortical bone and decrease in the signal of the bone marrow, which appears grey because of its involvement by the tumor (white arrows).

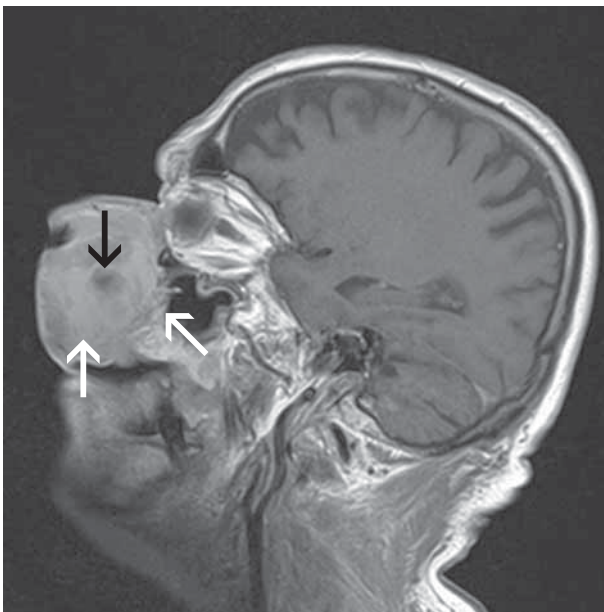


Fig. 3. Sagittal contrast-enhanced T1-weighted image shows malignant melanoma with a zone of necrosis (black arrow). Cutaneous and subcutaneous fat tissue, facial and perioral muscles are infiltrated by the tumor (arrows). The bone and cartilage structures of the nose are destroyed.

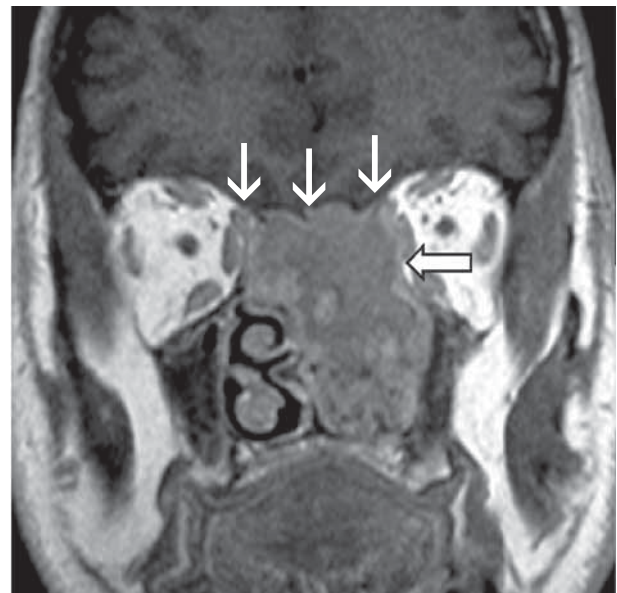


Fig. 5. Coronal contrast-enhanced T1-weighted image shows squamous cell carcinoma of ethmoid cells. Inhomogeneous tumor mass without intracranial extension is seen (white arrows). Intraorbital tumor propagation pressing medial orbicular muscle is shown (empty white arrow).

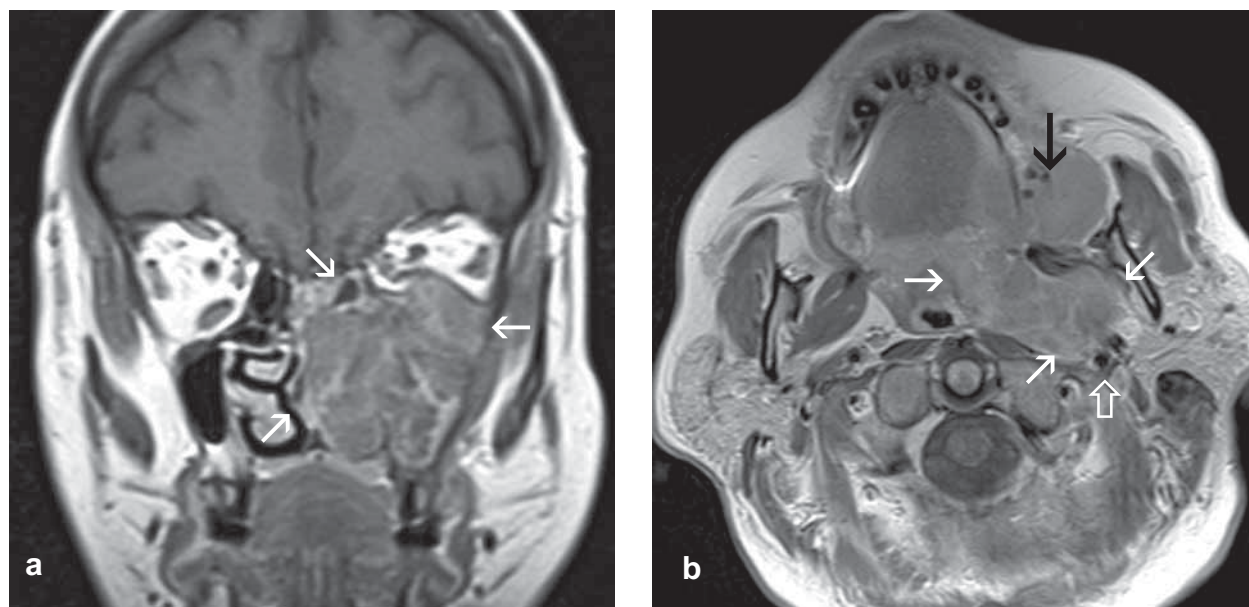


Fig. 6. Squamous cell carcinoma of the maxillary sinus: (a) coronal contrast-enhanced T1-weighted image showing tumor extension to the left nasal fossa, ethmoid cells and intraorbital propagation with dislocation of inferior orbicular muscle and optic nerve (white arrows); (b) axial contrast-enhanced T1-weighted image shows suppressed of carotid arteries due to tumor propagation to the carotid space (empty white arrow). The tumor spread to the buccal, parapharyngeal and pharyngeal spaces and pterygopalatine fossa (white arrows), and to bone structure of the maxilla and hard palate (black arrow).

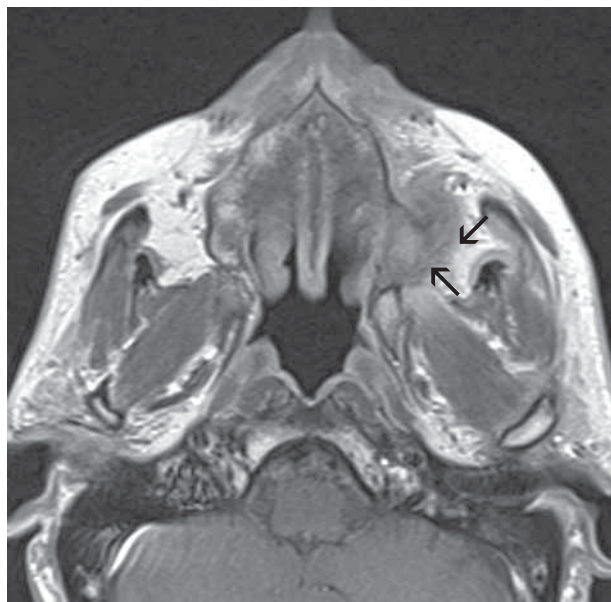


Fig. 7. Axial contrast-enhanced T1-weighted image shows squamous cell carcinoma of the gingival maxilla and hard palate. Involvement of branches of the superior alveolar nerve by the tumor (black arrows) is shown, which caused facial pain on the left side.

The extension of maxillofacial malignant tumor to neurovascular structures, fat tissue, muscles and anatomical spaces by MRI showed positive findings in 39 patients, which corresponded well with the intraoperative and histopathologic findings. On the analysis of perineural infiltration, MRI showed 91% sensitivity and 96.7% specificity. Tumor involvement of vascular structures was found in 22 patients, yielding a 91.6% specificity and 88% sensitivity. MRI showed 93.5% sensitivity and 90.9% specificity in the evaluation of intracranial extension, intraorbital propagation, and extension to pterygopalatine and infratemporal fossa and other surrounding anatomic spaces (Figs. 5-9).

Discussion

In daily practice at our hospital, we use multislice computed tomography (MSCT) in the analysis of malignant tumors of the maxillofacial region, which is complementary with MRI⁹. MSCT acquisition is much faster with multislice scanners, between 1-3 minutes including contrast administration. MSCT study is less time consuming than MR examination.

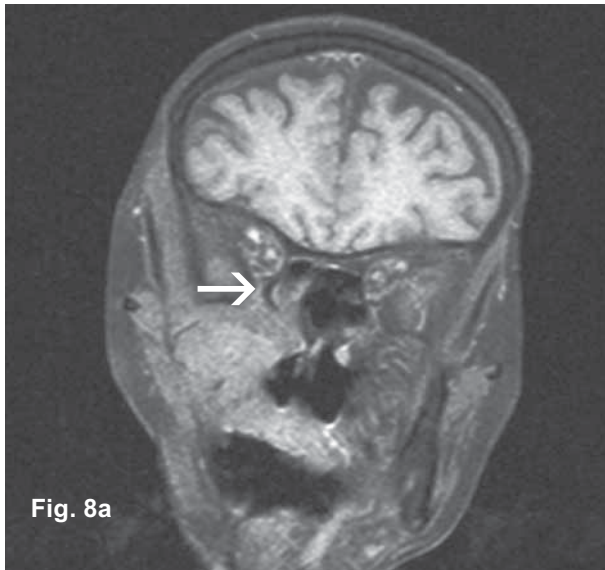


Fig. 8a

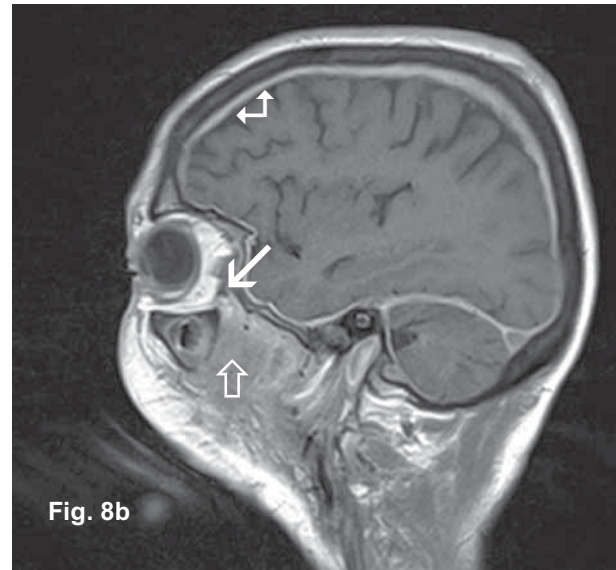


Fig. 8b

Fig. 8. Relapse of maxillary sinus squamous cell carcinoma 20 years after irradiation and surgery for tongue cancer: (a, b) coronal T1-weighted image with fat saturation and sagittal contrast-enhanced T1 weighted image show perineural infiltration through inferior orbital fissure (white arrows). Pterygomaxillary space and pterygopalatine fossa are involved by the tumor (empty white arrow). Thickened cranial dura mater is well contrast-enhanced after irradiation (left-up white arrow); (c) coronal STIR image shows high signal in mastoid cells (empty white arrow) due to perineural infiltration of mandibular nerve and dysfunction of motor tensor muscle of tympanic membrane.



Fig. 8c

On our MR machine, the average time is half an hour. The quality of MR image can be compromised by long time of examination due to swallowing artifacts.

In a study reported by Belkin *et al.*, persistent limitation in the head and neck MSCT analysis was caused by metal artifacts from dental restorative material¹⁰. Artifacts caused by metallic objects such as dental crowns, dental implants and metallic orthodontic appliances are a common problem in head and neck MRI¹¹. We had five patients with these artifacts. The patients with dentures that can be taken out, or patients without metal dental fillings are not affected by these problems and analysis was much better.

Because of a slightly superior spatial resolution of MSCT, early cortical involvement by tumor was often more easily seen by MSCT than by MRI¹². The MSCT evaluation of marrow involvement required recognition of a subtle increase in bone marrow density¹². In the present study, the high signal involvement of cortical bone and inhomogeneous decrease of bone marrow signal pointed to the diagnosis of bone infiltration (Figs. 2 and 4). Our MRI results were sensitive for both medullary and cortical bone involvement.

Several authors compared MRI and MSCT in the preoperative evaluation of osteosarcoma and primary bone tumors¹². They agree that MRI is superior to MSCT for determining tumor margins towards normal adjacent muscle, while MSCT is considered superior for the evaluation of subtle cortical changes and identification and characterization of mineralized tu-

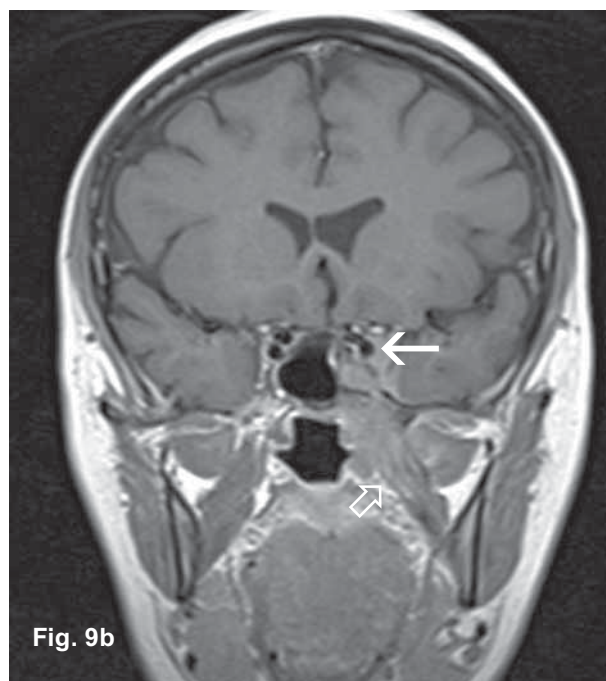
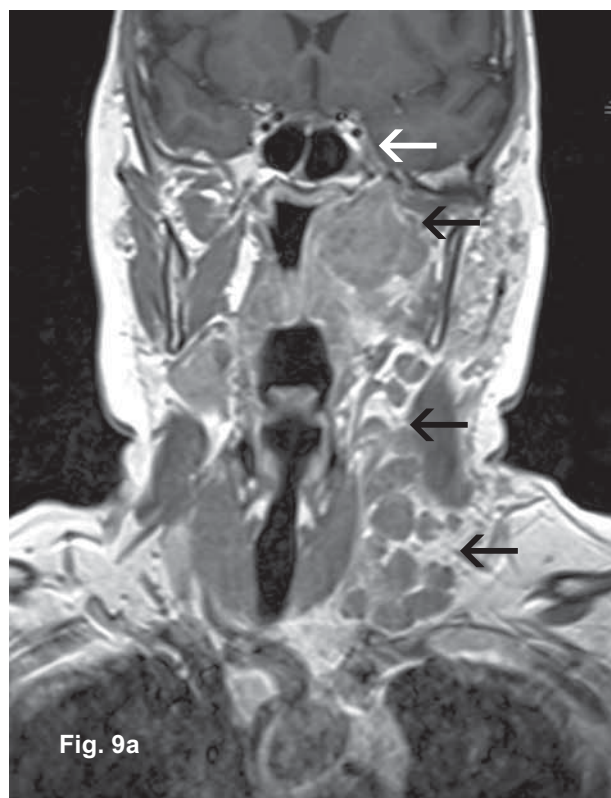


Fig. 9b

mor matrix¹². In their ability to determine intramedullary tumor extent, MRI and MSCT are usually comparable, but generally, MSCT will define better the margins of tumors that are highly sclerotic, and MRI can be preferable for detection of osteolytic lesions¹³. In the evaluation of bone involvement, MSCT has advantages in tumor osteosclerosis detection, which is a well known limitation of MRI¹³.

Fig. 9. Highly aggressive sinonasal undifferentiated carcinoma: (a, b) coronal contrast-enhanced T1 weighted images show tumor extent to the masticator space, masticatory muscles and lymph nodes of the head and neck (black arrows). Perineural infiltration along the third division of the trigeminal nerve, through oval hole involving the left cavernous sinus, (white arrow). Denervation atrophy of the masticatory muscles due to perineural infiltration (white arrow); (c) coronal contrast-enhanced T1 weighted image shows perivascular involvement of the internal carotid artery in the neck and cavernous part (white arrows). Blood vessel was easily identified as a black area of the signal void, 'flow void' phenomenon (empty white arrow).



Fig. 9c

tent of tumor invasion into the mandible and maxilla and further extension into the adjacent face and neck spaces and structures are causes of special concerns and may lead to poor prognosis¹⁶. Involvement of the pterygopalatine fossa and masticator space enables invasion along the neurovascular bundles into the cavernous sinus *via* maxillary and mandibular nerves¹⁶. MRI showed excellent presentation of tumor extension into anatomical spaces (Figs. 5-9).

MRI improved soft tissue visualization without the use of intravenous contrast medium, and distinguishes blood vessels and nerves from adjacent soft tissue and tumor lesions¹⁷. Blood vessel was easily identified as a black area of signal void, 'flow void' phenomenon¹⁷. In spite of this MRI advantage, in our study we used paramagnetic intravenous contrast media to achieve better contrast resolution.

MRI demonstrated advantage compared to MSCT in the evaluation of neurovascular structures from adjacent soft tissues¹⁸. MRI is more sensitive and specific than MSCT in detecting perineural spread¹⁹. MRI excellently presented perineural spread and vascular involvement caused by tumor (Figs. 7-9).

Appropriate assessment of the extent of tumor infiltration to the surrounding bone, neurovascular and other soft tissue structures is critical for proper planning of surgical treatment, which is often mutilating for the patient. The value of our study is to help surgeons choose an appropriate therapeutic option

Conclusion

Malignant tumors of the maxillofacial region are relatively rare, but, for radiologists, their differentiation and evaluation is not easy because many different types of tumors are present in this region. In our study that comprised 42 patients we analyzed the possibilities of MRI in the detection, diagnosis and differential diagnosis of malignant tumors of the maxillofacial region.

MRI results were compared with intraoperative and histopathologic findings and were statistically analyzed. We determined the specificity of MRI in assessing tumor localization (84%), establishing the zone of necrosis (92.8%) and hemorrhage (92.8%), bone involvement (85.7%), perineural infiltration (96.7%), involvement of vascular structures (88%), and tumor spread to the bone (88.2%) and soft tissue

structures and anatomic spaces (90.9%). The sensitivity of MRI was as follows: localization 94.4%, necrotic zones 93%, hemorrhage 93.3%, perineural infiltration 91%, involvement of vascular structures 91.6%, bone involvement 91.4%, extension of soft tissue tumors to bone structures 94.4%, and extension of soft tissue tumors to the surrounding soft tissue and anatomic spaces 93.5%.

MRI is a relatively new radiological imaging method that has not yet found routine application in the detection and assessment of malignant tumors of the maxillofacial region. The results of our study confirmed the high value of MR detection, differentiation and assessment of maxillofacial region malignant tumors. At our hospital, MRI has been established in preoperative treatment in some patients and our intention is to introduce MRI as a routine preoperative examination in all patients with tumors of the maxillofacial region.

References

1. BARNES L, EVESON JW, REICHAERT P, SIDRANSKY D. World Health Organisation classification of tumors. Pathology & Genetics. Head and neck tumors. Lyon: International Agency for Research on Cancer Press, 2005.
2. WEBER AL, BUI C, KANEDA T. Malignant tumors of the mandible and maxilla. *Neuroimaging Clin North Am* 2003; 13:509-24.
3. RAJESH A, KHAN A, KENDALL C, HAYTER J, CHERRYMAN G. Can magnetic resonance imaging replace single photon computed tomography and computed tomography in detecting bony invasion in patients with oral squamous cell carcinoma. *Br J Oral Maxillofac Surg* 2008;46:11-4.
4. LUPINETTI AD, ROBERTS DB, WILLIAMS MD, KUPFERMAN ME, ROSENTHAL DI, DeMONTE F, *et al.* Sinonasal adenoid cystic carcinoma. *Cancer* 2007;110:2726-31.
5. LARSON DL, LARSON JD. Head and neck melanoma. *Clin Plast Surg* 2010;37:73-3.
6. FERNANDES R, NIKITAKIS GN, PAZOKI A, ORD AR. Osteogenic sarcoma of the jaw: a 10-year experience. *Am Assoc Oral Maxillofac Surg* 2007;65:1286-91.
7. CHINDIA LM. Osteosarcoma of the jaw bones. *Oral Oncol* 2001;37:545-7.
8. YEO JK, SOO AI, GYE-YEON L, HO JC, HYUN JP, MIN SK, *et al.* Myxoid chondrosarcoma of the sinonasal cavity in a child: a case report. *Korean J Radiol* 2007;8:452-5.
9. CHAVDA VS, OLLIFF JFC. The sinuses. In: SUTTON D, ed. *Textbook of radiology and imaging*. Vol 2, 7th rev. ed. Fali grad: Elsevier, Churchill Livingstone, 2003;1519-29.

10. BELKIN AB, PAPAGEORGE BM, FAKITSAS J, BANKOFF M. A comparative study of magnetic resonance imaging *versus* computed tomography for the evaluation of maxillary and mandibular tumors. *J Oral Maxillofac Surg* 1988;46:1039-47.
11. COSTA A, APPENZELLER S, YASUDA C, PEREIRA F, ZANARDI V, CENDES F. Artifacts in brain magnetic resonance imaging due to metallic dental objects. *Med Oral Pathol Oral Cir Bucal* 2009;20:Pub Med PMID:19300374.
12. ZIMMER WD, BERQUIST TH, Mc LEOD RA, SIM FH, PRITCHARD DJ, SHIVES TC, *et al.* Bone tumors: magnetic resonance imaging *versus* computed tomography. *Radiology* 1985;155:709-18.
13. AISEN AM, MARTEL W, BRAUNSTEIN EM, Mc MILLIN KI, PHILLIPS WA, KLING TF. MRI and CT evaluation of primary bone and soft-tissue tumors. *Am J Radiol* 1986;146:749-56.
14. Mc ENERY KW, MURPHY WA. Magnetic resonance imaging. In: RESNICK D, ed. *Bone and joint imaging*. 2nd ed. Philadelphia: Saunders, 1996; 84-92.
15. KASSEL EE, KELLER MA, KUCHARCZYK W. MRI of the floor of the mouth, tongue and oropharynx. *Radiol Clin North Am* 1989;27:331-51.
16. KIMURA Y, SUMI M, ARIJI Y, ARIJI Y, NAKAMURA T. Deep extension from carcinoma arising from the gingiva: CT and MR imaging features. *AJN Am J Neuroradiol* 2002;23:468-472.
17. WILLIAMS LS, MANCUSO AA, MENDENHALL WA. Perineural spread of cutaneous squamous and basal cell carcinoma: CT and MR detection and its impact on patient management and prognosis. *Int Radiat Oncol Biol Phys* 2001;49:1061-9.
18. GINSBERG LW. MR imaging of perineural tumor spread. *Magn Reson Imaging Clin North Am* 2004;14:663-77.
19. HANNA E, VURAL E, PROKOPAKIS E, CARRAU R, SNYDERMAN C, WEISSMAN J. The sensitivity and specificity of high-resolution imaging in evaluating perineural spread of adenoid cystic carcinoma to the skull base. *Arch Otolaryngol Head Neck Surg* 2007;133:541-5.
20. HARNBERGER HC, HUDGINS PA, WIGGINS RH, HUDGINS PA, MICHEL MA, DAVIDSON HC, *et al.* *Diagnostic imaging: head and neck*. 1st ed. Canada grad?: Amirsys, 2008.

Sažetak

MAGNETSKA REZONANCIJA U DIJAGNOSTICI ZLOČUDNIH TUMORA MAKSILOFACIJALNOG PODRUČJA

D. Podoreški, I. Krolo, M. Ivkić, M. Marotti, V. Kosović i K. Višković

Magnetska rezonancija (MRI) je radiološka slikovna metoda koja još uvijek nije pronašla rutinsku primjenu u otkrivanju i procjeni malignih tumora maksilofacijalnog područja. Svrha ove studije je bila pokazati vrijednost MRI u otkrivanju, dijagnostici i diferencijalnoj dijagnostici malignih tumora maksilofacijalnog područja. Ova prospektivna studija uključila je 42 bolesnika s klinički potvrđenim zloćudnim tumorom maksilofacijalnog područja. Svi bolesnici su bili obrađeni pomoću MRI. Analizirala se lokalizacija, dimenzije i struktura tumora, zahvaćenost koštanih struktura, utjecaj na neurovaskularne strukture, proširenost na okolne mekotkivne strukture i prostore. Rezultati su se uspoređivali s patohistološkim i intraoperacijskim nalazom kao „zlatnim“ standardom. MRI je prikazao sve klinički potvrđene tumore. U procjeni lokalizacije tumora osjetljivost je bila 94,4%; zone nekroze 93%; zone krvarenja 93,3%; te promjene koštane strukture 91,4%. U procjeni lokalizacije tumora specifičnost je bila 84%; zone nekroze 92,8%; zone krvarenja 92,8%; te promjene koštane strukture 85,7%. U procjeni zahvaćenosti koštanih struktura mekotkivnim tumorskim procesom osjetljivost MRI je bila 94,4%, a specifičnost 88,2%. Osjetljivost kod procjene perineuralne infiltracije je bila 91%, a utjecaja tumora na vaskularne strukture 91,6%. Specifičnost kod procjene perineuralne infiltracije je bila 96,7%, a utjecaja tumora na vaskularne strukture 88%. MRI je pokazao osjetljivost od 93,5% i specifičnost od 90,9% za intrakranijsku i intraorbitalnu propagaciju, prodor u pterigopalatinalnu udubinu i druge okolne anatomske prostore. Prednost MRI je u sposobnosti razlikovanja neuralnih i vaskularnih struktura bez primjene intravenskog kontrastnog sredstva. Naši rezultati su potvrdili vrlo važnu ulogu MRI u procjeni strukture tumora, koštanih promjena i proširenosti tumora u okolne strukture i prostore.

Ključne riječi: Novotvorine maksile – dijagnostika; Novotvorine maksile – radiografija; Magnetska rezonancija – upotreba; Invazivnost novotvorine – dijagnostika